Biomedicine & Pharmacotherapy 193 (2025) 118763

Contents lists available at ScienceDirect

Biomedicine & Pharmacotherapy

journal homepage: www.elsevier.com/locate/biopha

Repurposed membrane-targeting RS17053 eradicates MRSA persisters and enhances aminoglycoside killing

Seongeun Baek [a], Guijin Zou [b], Nakyung Lee [a], Jisoo Kang [a], Jae-Seok Kim [c], Wonhyo Seo [a], Huajian Gao [b], Wooseong Kim [a,*]

[a] College of Pharmacy, Graduate School of Pharmaceutical Sciences, Ewha Womans University, Seoul 03760, Republic of Korea
[b] Mechano-X Institute, Applied Mechanics Laboratory, Department of Engineering Mechanics, Tsinghua University, Beijing 100084, China
[c] Department of Laboratory Medicine, Kangdong Sacred Heart Hospital, Hallym University College of Medicine, Seoul 05355, Republic of Korea

ARTICLE INFO

Keywords:
Antibiotic-resistance
MRSA
Persisters
Membrane-active agents
Adjuvant
Drug repurposing

ABSTRACT

The rapid rise of methicillin-resistant *Staphylococcus aureus* (MRSA) and its ability to form antibiotic-tolerant persisters pose a major challenge to antimicrobial therapy. These metabolically dormant cells survive antibiotic exposure without genetic resistance, driving chronic and relapsing infections. Here, we characterize RS17053—a selective α1A-adrenoceptor antagonist— as a membrane-active compound with potent activity against both antibiotic-resistant and antibiotic-tolerant *S. aureus*. RS17053 disrupts bacterial phospholipid bilayers, causing membrane permeabilization, intracellular leakage, accumulation of reactive oxygen species, and subsequent cell death, while exhibiting minimal cytotoxicity toward mammalian cells. The compound shows no detectable resistance after prolonged exposure and synergistically enhances aminoglycoside potency by promoting drug uptake into MRSA persisters. In a *Caenorhabditis elegans* infection model, RS17053 protects hosts from lethal MRSA challenge. Collectively, these findings support RS17053 as an antimicrobial lead compound suitable for repurposing as both a direct-acting antimicrobial and an adjuvant to aminoglycosides for treating persistent MRSA infections.

1. Introduction

Staphylococcus aureus is a gram-positive pathogen responsible for several infections in both community and healthcare settings. Although most *S. aureus* infections are treatable with antibiotics, the emergence of drug-resistant strains has severely constrained therapeutic options. Particularly, the rise of methicillin-resistant *S. aureus* (MRSA), vancomycin-intermediate *S. aureus*, and vancomycin-resistant *S. aureus* (VRSA) has further complicated infection management, leading to persistently high disease burden despite advances in antimicrobial therapy [1]. Among major bacterial pathogens, *S. aureus* has exhibited the largest increase in antimicrobial resistance (AMR)-related mortality, with attributable deaths rising from 103,000 in 1990–196,000 in 2021 globally [2]. Although vancomycin, linezolid, and daptomycin remain frontline therapies for severe MRSA infections, the continued evolution of resistant strains underscores the urgent need for alternative treatments [3].

Beyond genetic resistance, *S. aureus* can survive antimicrobial treatment through phenotypic adaptations, forming persister cells—a metabolically dormant, nonreplicating subpopulation that can transiently tolerate high antibiotic concentrations [4,5]. In contrast to genetically resistant bacteria, persisters evade antibiotic killing primarily because of reduced metabolic activity, including diminished cell wall synthesis, nucleic acid replication, and protein translation, without heritable resistance mutations, rendering them largely refractory to conventional antibiotics [6]. Persisters exhibit tolerance to diverse classes of bactericidal antibiotics, including β-lactams, aminoglycosides, and fluoroquinolones, despite their distinct mechanisms of action [4,7,8]. Moreover, current antibiotic development is primarily focused on actively dividing cells, leaving nonreplicating persisters largely unaffected. This fundamental limitation highlights the necessity for the development of novel therapeutic strategies capable of eradicating both drug-resistant bacteria and their antibiotic-tolerant persisters.

Membrane-active agents are promising candidates for targeting bacterial persisters because membrane integrity is essential for bacterial viability regardless of metabolic or growth state [6,9,10]. Moreover,

* Correspondence to: Ewha Womans University, Pharmaceutical Science Bldg B-315, 52 Ewhayeodae-gil, Seodaemun-gu, Seoul 03760, Republic of Korea
E-mail address: wooseong_kim@ewha.ac.kr (W. Kim).

https://doi.org/10.1016/j.biopha.2025.118763
Received 20 August 2025; Received in revised form 28 October 2025; Accepted 7 November 2025
Available online 10 November 2025
0753-3322/© 2025 The Authors. Published by Elsevier Masson SAS. This is an open access article under the CC BY-NC license (http://creativecommons.org/licenses/by-nc/4.0/).

membrane modification is a complex, multigenic process that cannot be achieved through a single mutation, making bacteria less likely to develop resistance to membrane-disrupting antibiotics [9]. However, many of these agents lack selectivity for bacterial over mammalian membranes, leading to cytotoxicity that restricts their clinical application. For instance, although α-mangostin, a polyphenolic xanthonoid, and NH125, a small-molecule antimicrobial, can effectively kill MRSA via membrane disruption, both cause significant hemolysis [11,12]. Furthermore, not all membrane-active agents that kill actively growing bacteria are effective against persisters. For example, the FDA-approved lipopeptide daptomycin and the small molecule PQ401, both of which target bacterial lipid bilayers, fail to eradicate MRSA persisters [13–15]. These limitations highlight the need for membrane-active agents that combine potent antipersister activity with selective bacterial membrane targeting.

Here, we report RS17053, a small molecule originally developed as a selective α1A-adrenoceptor antagonist, as a potent antipersister agent. RS17053 selectively disrupts bacterial membranes, eradicates MRSA persisters, and synergizes with aminoglycosides. Through molecular dynamics simulations and mechanistic assays, we define its membrane-disruptive mode of action. In a *Caenorhabditis elegans* infection model, RS17053 significantly improves host survival, underscoring its potential for repurposing as both an antimicrobial and an aminoglycoside adjuvant.

2. Materials and methods

2.1. Bacterial strains and growth conditions

The bacterial strains used in this study are described in the Supporting Information. *S. aureus* strains were cultured in tryptic soy broth (TSB) (BD, Franklin Lakes, NJ, USA), whereas *E. faecalis* and *E. faecium* were grown in brain–heart infusion broth (BHI) (BD, Franklin Lakes, NJ, USA). *K. pneumoniae, A. baumannii, P. aeruginosa,* and *E. aerogenes* were cultured in Lennox broth (LB) (BD, Franklin Lakes, NJ, USA). Overnight cultures were prepared by inoculating a single colony of each bacterial strain into 5 mL of the appropriate broth, followed by incubation at 37 °C for 18–24 h with constant shaking at 250 rpm. To obtain MRSA MW2 cells in the exponential growth phase, overnight cultures were diluted 1:10,000 into 25 mL of fresh TSB within a 250 mL Erlenmeyer flask and incubated at 37 °C with shaking at 250 rpm until the optical density at 600 nm (OD600) reached 0.2.

2.2. Antimicrobial agents and chemicals

Vancomycin, gentamicin, and ciprofloxacin were obtained from Sigma-Aldrich (St. Louis, MO, USA). RS17053 and daptomycin were purchased from R&D Systems (Minneapolis, MN, USA). RS17053 was dissolved in dimethyl sulfoxide (DMSO), and ciprofloxacin was dissolved in 0.1 N hydrochloric acid (HCl). All other compounds were dissolved in double-distilled water (ddH_2O). Stock solutions for all the agents were prepared at a concentration of 10 mg/mL and stored according to the manufacturer's instructions.

2.3. Antimicrobial compound screening

Screening for MRSA growth-inhibitory compounds was conducted as described previously [14]. Detailed procedures are provided in the Supporting Information.

2.4. Determination of the minimum inhibitory concentration (MIC)

The MICs of the antibacterial agents were determined using the standard microbroth dilution method, following Clinical and Laboratory Standards Institute guidelines [16]. Bacterial growth was defined as an OD600 value of $\geq$ 0.1. The experiments were independently repeated three times.

2.5. Exponential-phase cell-killing kinetic assays

In total, 500 μL of the exponential-phase *S. aureus* MW2 cell suspension in TSB medium was dispensed into a deep 96-well plate (Bioneer, Daejeon, Korea; cat. no. 90062) containing 500 μL of the test compounds at the indicated concentrations in TSB medium. The plate was incubated at 37 °C with shaking at 450 rpm. At hourly intervals, aliquots were collected, serially diluted 1:10 using phosphate-buffered saline (PBS), and 5 μL of each dilution was spot-plated onto Cation-adjusted Mueller Hinton broth (CaMH) agar plates. After overnight incubation at 37 °C, the colony-forming units (CFUs) were counted. The assay was performed in triplicate.

2.6. Serial passage resistance development assay

Serial passaging was performed over 15 consecutive days following a modified version of a previously established protocol [17]. Detailed methods are shown in the Supporting Information.

2.7. Checkerboard assay

Two-fold serial dilutions of RS17053 and each antibiotic were prepared in CaMHB. Subsequently, 50 μL of each dilution was added to the wells of a 96-well plate, followed by 50 μL of *S. aureus* MW2, adjusted to 1×10^6 CFU/mL. The plate was incubated at 37 °C for 24 h, after which bacterial growth was measured at OD600 using a Cytation 5 Cell Imaging Multi-Mode Reader (BioTek, USA). Growth was defined as an OD600 of $\geq$ 0.1. The interaction between agents was assessed using the fractional inhibitory concentration index (FICI), calculated as the sum of the MIC of each agent in combination divided by its MIC alone. A lower FICI indicates a stronger interaction, with synergy defined as $\leq$ 0.5, indifference as $>$ 1 to $\leq$ 4, and antagonism as $>$ 4 [18]. All assays were performed in triplicate.

2.8. Caenorhabditis elegans infection and toxicity assay

C. elegans-MRSA infection and toxicity assays were performed with slight modifications to previously described methods [19]. Detailed materials and procedures are provided in the Supporting Information.

2.9. Transmission electron microscopy (TEM)

TEM imaging was performed at the Ewha Medical Research Institute using a Hitachi H-7650 microscope. Detailed methods are described in the Supporting Information.

2.10. Intracellular reactive oxygen species (ROS) level evaluation

Intracellular ROS levels in *S. aureus* MW2 were determined using the fluorescent probe carboxy-H2DCFDA (Invitrogen, Carlsbad, CA, USA; cat. no. C400), prepared as a 10 mM stock solution. Bacterial cells were grown in CaMH medium to an OD600 of approximately 1.0 and then incubated with 10 μM carboxy-H2DCFDA, which fluoresces upon oxidation by ROS. Next, 50 μL of the treated cells were added to the wells of a black, clear-bottom 96-well plate containing RS17053 at the indicated concentrations. Fluorescence intensity was monitored over 6 h using a Cytation 5 Cell Imaging Multi-Mode Reader, with excitation and emission wavelengths of 490 nm and 520 nm, respectively. Bacterial growth was simultaneously measured by OD600, and fluorescence intensity was normalized to the corresponding OD600 values. All measurements were performed in triplicate.

2.11. Estimation of the intracellular NADH/NAD$^+$ ratio

The intracellular NADH/NAD$^+$ ratio in *S. aureus* ATCC 29213 was measured using a modified version of a previously described protocol [20]. Bacterial cells were cultured in TSB medium to an OD600 of approximately 0.2 and then washed three times with PBS and resuspended in PBS containing 2 μM resazurin sodium salt (Sigma-Aldrich, St. Louis, MO, USA; cat. no. R7017) and 0.4 % glucose. Subsequently, 50 μL of the bacterial suspension was added to each well of a 96-well plate, followed by 50 μL of RS17053 or the indicated antibiotics. Fluorescence intensity was measured every 10 min for 2 h using a Cytation 5 Multi-Mode Reader with excitation at 530 nm and emission at 590 nm. Fluorescence values were normalized to OD600 to account for differences in bacterial density. All experiments were performed in triplicate.

2.12. Membrane depolarization and permeability assays

Membrane depolarization was evaluated using the fluorogenic dye 3,3'-dipropylthiadicarbocyanine iodide [DiSC3(5)] (Sigma-Aldrich, St. Louis, MO, USA; cat. no. 43608), which detects changes in the proton motive force (PMF). Membrane permeabilization was assessed using the fluorescent dye SYTOX Green (ThermoFisher Scientific, USA;cat. no. S7020), which selectively penetrates cells with compromised membranes. Detailed methods for each assay are provided in the Supporting Information.

2.13. Persister preparation

Persister cells of *S. aureus* MW2 were generated using two methods: stationary-phase induction and arsenate induction [14,17]. To prepare stationary-phase persisters, an overnight culture was diluted 1:200 into 50 mL of fresh TSB in a 250-mL Erlenmeyer flask and incubated at 37°C with shaking at 250 rpm for 24 h. *S. aureus* MW2 cells in the stationary phase are known to consist predominantly of persisters [17]. To generate arsenate-induced persisters, exponential-phase cells were treated with 5 mM sodium arsenate and incubated for 30 min at 37 °C with shaking at 250 rpm [14]. In both cases, antibiotic tolerance was confirmed by the absence of a significant reduction in CFU/mL after a 4-h exposure to 100 × MIC of vancomycin, gentamicin, or ciprofloxacin.

2.14. Intracellular component leakage assays

Intracellular ATP and protein leakage were measured using the RealTime-Glo™ Extracellular ATP Assay kit (Promega, USA) and the Micro BCA Protein Assay kit (ThermoFisher Scientific, USA) according to the manufacturers' instructions. Detailed procedures are provided in the Supporting Information.

2.15. Membrane lipid binding assay

The interaction between RS17053 and membrane lipid components was evaluated by assessing MIC changes using a checkerboard microdilution assay. Detailed procedures are described in the Supporting Information.

2.16. All-atom molecular dynamics (MD) simulations

Molecular dynamics (MD) simulations were conducted to investigate the interaction between RS17053 and a model bacterial plasma membrane, following previously described methodologies [8]. Detailed simulation procedures are provided in the Supporting Information.

2.17. Hemolysis assay

Hemolytic activity was measured using human red blood cells and serial dilutions of RS17053 hydrochloride, with hemoglobin release quantified spectrophotometrically. The method followed previously described protocols [14] with minor modifications as detailed in the Supporting Information.

2.18. Biofilm persister killing assay

S. aureus MW2 biofilm persisters were prepared by diluting an overnight culture 1:200 in TSB supplemented with 0.2 % glucose and 3 % NaCl. Then, 1 mL of the diluted culture was added to each well of a 24-well plate containing a 13-mm mixed cellulose ester membrane (GSWP01300; EMD Millipore, USA) and incubated statically at 37°C for 24 h to allow biofilm formation. The membranes were then washed three times with 1 mL of PBS to remove planktonic cells. Subsequently, 1 mL of PBS containing the indicated concentrations of RS17053 or antibiotics was added to each well, followed by a 24-h incubation at 37 °C. After treatment, the membranes were washed three times with PBS and transferred to 1.5-mL microcentrifuge tubes containing 1 mL of PBS. The tubes were sonicated for 10 min in a Branson ultrasonic bath to detach the biofilm-associated cells. The resulting suspensions were serially diluted tenfold in PBS and spot-plated onto CaMH agar plates. After overnight incubation at 37 °C, colony-forming units (CFUs) were enumerated to quantify the surviving cells.

2.19. Gentamicin-Texas red uptake assay

The uptake of Texas Red-conjugated gentamicin (GTTR) was measured as previously described, with minor modifications (Heo et al., 2024). GTTR (AAT Bioquest, Pleasanton, CA, USA; cat. no. 24300) was dissolved in DMSO to prepare a 5 mg/mL stock solution. MRSA persister cells were incubated with 16 μg/mL GTTR and the indicated concentrations of RS17053 at room temperature for 1 h. After incubation, the cells were washed three times with PBS, and 100 μL of the washed suspension was transferred to a black, clear-bottom 96-well plate (Greiner Bio-One, cat. no. 665090). Fluorescence intensity was recorded using a Cytation 5 Cell Imaging Multi-Mode Reader with excitation and emission wavelengths of 589 and 615 nm, respectively. All experiments were performed in triplicate.

3. Results

3.1. RS17053 exhibits antimicrobial potency against antibiotic-resistant gram-positive bacteria

We identified RS17053 (Fig. 1A) as a hit from a previous compound library screen for anti-MRSA activity [14]. RS17053 was selected for further investigation because of its established biological activity and reported lack of acute toxicity in a rat model [21–23], indicating its potential for repurposing as an antimicrobial agent. To confirm its anti-MRSA activity, we determined that the MIC of RS17053 against *S. aureus* MW2 was 8 μg/mL (Table 1). RS17053 exhibited bactericidal activity, reducing *S. aureus* MW2 viability by 2 logs within 4 h at 10 μg/mL—faster than vancomycin but slower than daptomycin at the same concentration (Fig. 1B). RS17053 also demonstrated antimicrobial activity against *E. faecium* (MIC: 4 μg/mL) but displayed minimal or no activity against gram-negative bacteria, including *K. pneumoniae*, *A. baumannii*, *P. aeruginosa*, and *E. aerogenes* (Table 1).

Further, we assessed its activity against multidrug-resistant gram-positive pathogens. RS17053 displayed MIC values of 4 or 8 μg/mL against multiple MRSA clinical isolates, VRSA, *E. faecalis*, and vancomycin-resistant *Enterococcus* strains (Table 2). Collectively, these findings suggest that RS17053, previously characterized as a selective α1A-adrenergic receptor antagonist, possesses potent antimicrobial activity against several antibiotic-resistant gram-positive bacteria.

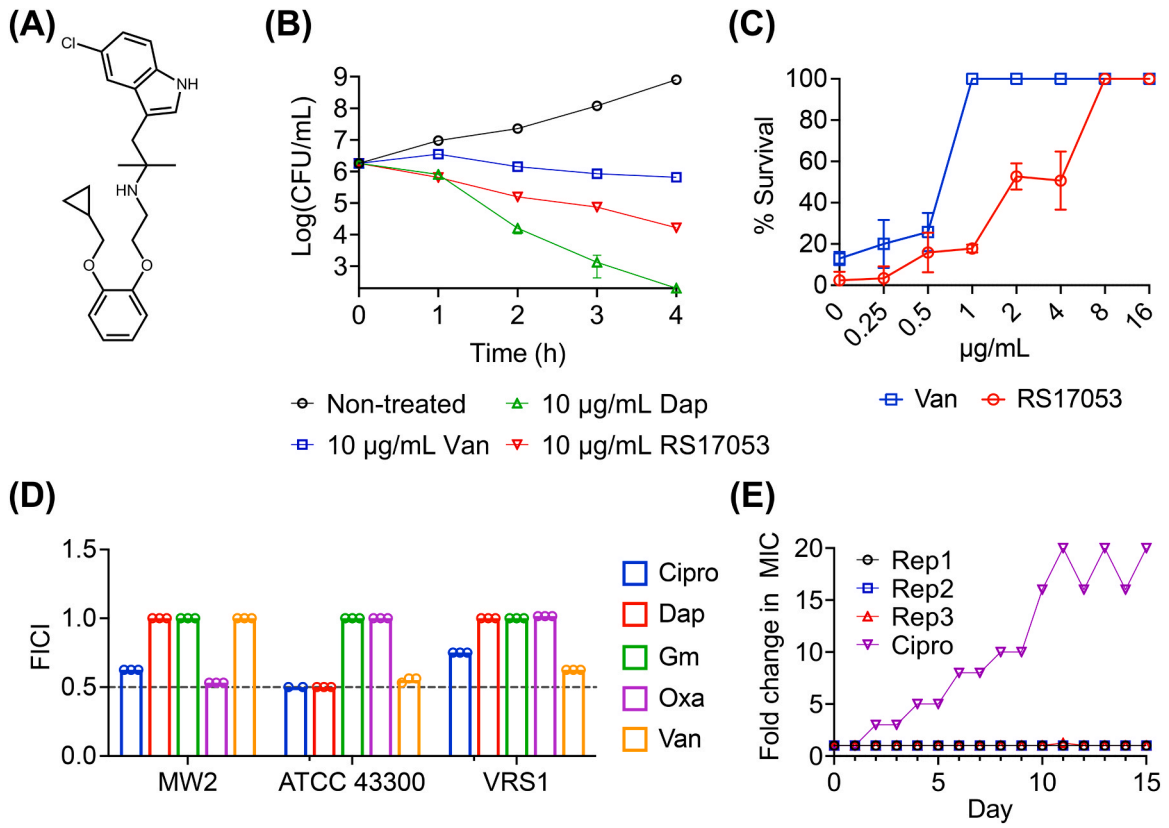


Fig. 1. RS17053 exhibits potent anti-**MRSA** activity without inducing resistance and does not antagonize other antibiotics. (A) Chemical structure of RS17053. (B) Exponentially growing MRSA MW2 cells were treated with RS17053, vancomycin (Van), or daptomycin (Dap) for 4 h. Bacterial survival was measured at 1-h intervals, with a detection limit of 2×10^2 CFU/mL. Error bars represent mean ± SD (n = 3). (C) *In vivo* efficacy of RS17053 was evaluated using a *C. elegans* MRSA infection model, with vancomycin (Van) as a positive control. (D) Checkerboard microdilution assays were performed to assess interactions between RS17053 and vancomycin (Van), oxacillin (Oxa), gentamicin (Gm), daptomycin (Dap), or ciprofloxacin (Cipro). Interactions were quantified using the fractional inhibitory concentration index (FICI) and defined as synergistic (FICI ≤ 0.5), additive (0.5 < FICI ≤ 1), indifferent (1 < FICI ≤ 4), and antagonistic (FICI > 4). Individual data points are shown (n = 3). (E) Resistance development was evaluated over 15 days by serial passage of MRSA MW2 in the presence of either ciprofloxacin (Cipro) or RS17053. Rep 1, 2, and 3 indicate biological replicates treated with RS17053.

Table 1
Minimum inhibitory concentration (μg/mL) of RS17053 against ESKAPE strains.

Strains	RS17053	Oxa	Van	Dap	Gm	Cipro
S. aureus MW2	8	32	1	1	0.5	0.25
E. faecium E007	4	> 64	0.5	8	> 64	64
K. pneumoniae WGLW2	> 64	> 64	> 64	> 64	1	0.0625
A. baumannii ATCC 17978	64	> 64	> 64	> 64	0.5	0.5
P. aeruginosa PA14	> 64	> 64	> 64	> 64	4	< 0.0625
E. aerogenes ATCC 13048	> 64	> 64	> 64	> 64	0.25	< 0.0625

Oxa: oxacillin, Van: vancomycin, Dap: daptomycin, Gm: gentamicin, Cipro: ciprofloxacin

3.2. RS17053 rescues C. elegans from MRSA and shows low resistance potential

We evaluated the *in vivo* efficacy of RS17053 using the well-established *C. elegans* whole-animal infection model [24]. RS17053 improved the survival of infected worms in a dose-dependent manner, rescuing 50 % at 2–4 μg/mL and achieving complete protection at 8 μg/mL, corresponding to its MIC against *S. aureus* MW2 (Fig. 1C). These findings indicate that RS17053 can confer *in vivo* protection, consistent with its antimicrobial activity observed *in vitro*.

Next, we examined potential interactions between RS17053 and conventional antibiotics against MRSA and VRSA strains using a checkerboard assay. In the MRSA strain MW2, RS17053 displayed additive interactions with oxacillin, gentamicin, ciprofloxacin, vancomycin, and daptomycin (0.5 < FICI ≤ 1; Fig. 1D). In the MRSA strain ATCC 43300, RS17053 synergized with ciprofloxacin (FICI = 0.5) and showed additive effects with the remaining agents. In the VRSA strain VRS1,

Table 2
Minimum inhibitory concentration (μg/mL) of RS17053 against multidrug-resistant gram-positive pathogens.

Bacteria	Strain	RS17053	Oxa	Van	Dap	Gm	Cipro
S. aureus	ATCC 33591	8	> 64	1	0.5	2	0.25
	ATCC 43300	8	32	1	1	64	0.25
	HLSA 16278	8	> 64	1	1	0.25	1
	HLSA 17064	8	> 64	0.5	1	> 64	> 64
	HLSA 17078	8	64	0.5	0.5	64	16
	HLSA 18380	8	> 64	0.5	1	0.25	16
	HLSA 18807	8	> 64	0.5	0.5	0.25	64
	HLSA 18840	8	> 64	1	1	> 64	32
	HLSA 18883	8	> 64	0.5	1	> 64	> 64
	HLSA 18888	8	> 64	0.5	0.5	> 64	> 64
	HLSA 20835	8	> 64	1	1	0.5	64
	VRS1	8	> 64	> 64	1	64	64
E. faecalis	MMH594	4	32	1	8	> 64	0.125
E. faecium	C68*	8	> 64	> 64	32	> 64	> 64
	WB312*	8	> 64	64	32	64	> 64
	WC176*	8	> 64	> 64	32	> 64	4

Oxa: oxacillin, Van: vancomycin, Dap: daptomycin, Gm: gentamicin, Cipro: ciprofloxacin

RS17053 demonstrated additive effects with gentamicin, ciprofloxacin, vancomycin, and daptomycin, and an indifferent interaction with oxacillin (FICI = 1.02). These findings confirm that RS17053 does not antagonize the activity of the tested antibiotics, supporting its use in combination therapy.

To assess the likelihood of resistance development, we subjected *S. aureus* MW2 to sub-MIC levels of RS17053 over 15 days, with ciprofloxacin, a DNA gyrase inhibitor, serving as a control. Ciprofloxacin treatment led to a 20-fold MIC increase, indicating the emergence of resistance. In contrast, RS17053 did not lead to any measurable MIC change (Fig. 1E), suggesting a low propensity for resistance development.

3.3. RS17053 compromises MRSA membrane integrity

To examine the effects of RS17053 on MRSA morphology, we performed TEM on exponential-phase *S. aureus* MW2 cells treated with RS17053 at 4 × MIC for 2 h. TEM images revealed intracellular mesosome-like structures and abnormal cell division (Fig. 2A), which are characteristic features of membrane-disrupting antimicrobials [8,25]. These structural changes suggest that RS17053 compromises bacterial membrane integrity.

Given that the electron transport chain (ETC) is embedded within the membrane, its disruption can impair ETC function, reducing NADH consumption and leading to an increased NADH/NAD⁺ ratio. To test this hypothesis, we measured intracellular NADH/NAD⁺ levels in RS17053-treated MRSA cells. RS17053 at concentrations of 8 μg/mL or higher significantly elevated the NADH/NAD⁺ ratio (Fig. 2B), indicating potential ETC dysfunction. Moreover, ETC impairment often leads to electron leakage, triggering ROS accumulation [26]. In line with this, RS17053 caused a dose-dependent increase in ROS levels (Fig. 2C).

To further characterize its effects, we evaluated changes in the proton motive force (PMF), membrane permeability, and the leakage of intracellular contents. RS17053 treatment led to the release of the PMF-sensitive dye DiSC3(5), indicating membrane depolarization. Additionally, RS17053 at concentrations of at least 16 μg/mL induced the rapid uptake of SYTOX Green, a membrane-impermeable DNA-binding dye, confirming increased membrane permeability. Moreover, RS17053 triggered significant leakage of intracellular ATP and proteins from MRSA cells (Fig. 2F, G). Collectively, these findings demonstrate that RS17053 disrupts MRSA membrane integrity, compromising both membrane function and cellular homeostasis.

3.4. RS17053 interacts with and inserts into membrane phospholipid bilayers

To investigate the molecular interactions between RS17053 and bacterial membranes, we conducted all-atom MD simulations using a negatively charged lipid bilayer model comprising DOPC and DOPG at a 7:3 ratio, a well-established model to study bacterial membrane interactions [8,27]. The simulations revealed that RS17053 initially binds at the lipid–water interface via electrostatic interactions between its indole NH group and the negatively charged DOPG head groups (Fig. 3A, Video S1). As RS17053 embeds further into the membrane, its

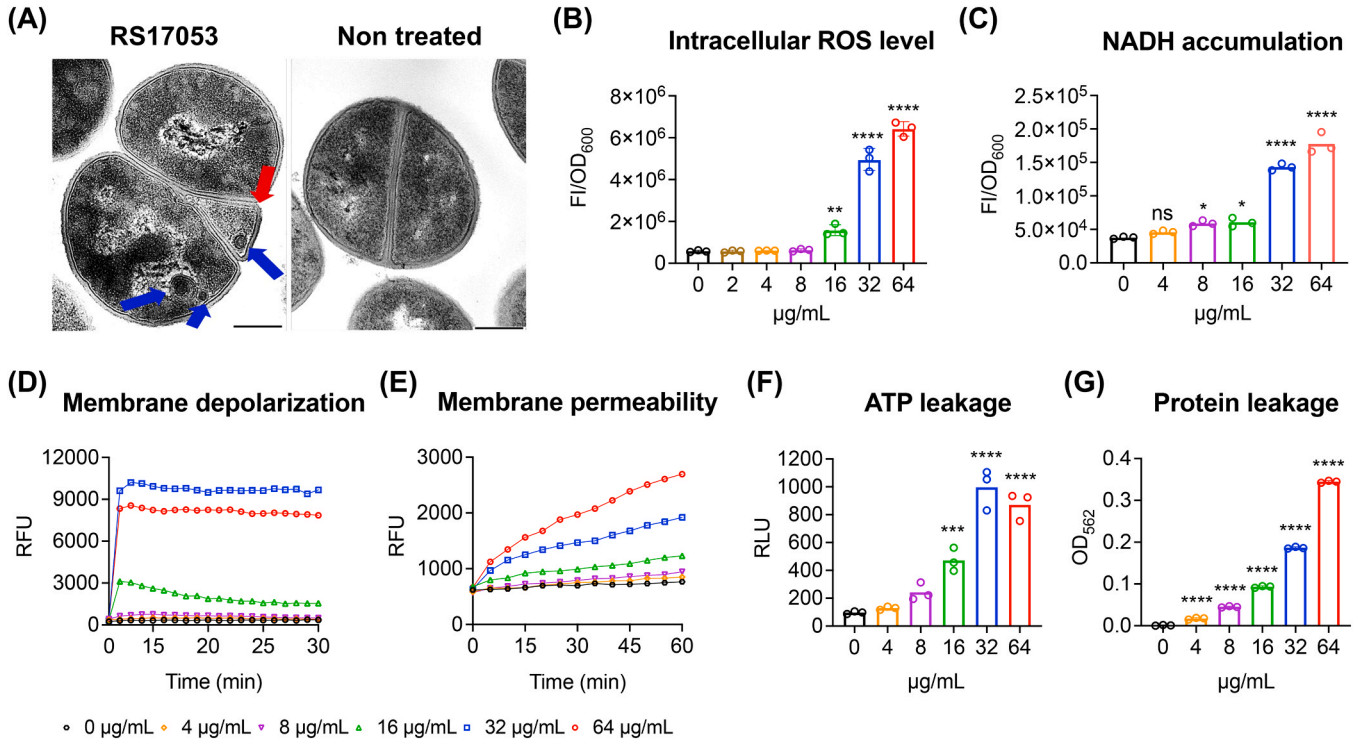


Fig. 2. RS17053 kills growing **MRSA** by disrupting membrane integrity. (A) Transmission electron microscopy (TEM) images exponentially growing MRSA MW2 cells treated with 4 × MIC RS17053 show mesosome-like structures (blue arrows) and abnormal cell division (red arrow), in contrast to untreated controls. Scale bar: 1 μm. (B) Intracellular reactive oxygen species (ROS) levels were measured 6 h after RS17053 treatment using the fluorescent probe carboxy-H_2DCFDA. (C) Intracellular NADH levels were quantified using a resazurin reduction assay, indicating NADH accumulation following treatment. (D) Proton motive force (PMF) dissipation was assessed using the membrane potential-sensitive dye $DiSC_3(5)$, revealing RS17053-induced membrane depolarization. (E) Membrane permeability was evaluated by measuring SYTOX Green fluorescence 60 min post-treatment, which increases upon entry into cells with compromised membranes. (F) Cellular ATP leakage was quantified 1 h post-treatment using an ATP luminescence assay, indicating RS17053-induced loss of intracellular ATP. (G) Protein leakage from MRSA MW2 cells was determined 1 h post-treatment using a micro-BCA protein assay, showing RS17053-induced protein release. In panels (B) and (C), FI represents fluorescence intensity; in panels (D) and (E), RFU represents relative fluorescence units; and in panel (F), RLU denotes relative luminescence units. In panels (B), (C), (F), and (G), each data point represents an independent biological replicate. Error bars indicate mean ± SD (n = 3). Statistical significance was evaluated by one-way ANOVA followed by Tukey's post-hoc test (*$p < 0.05$, **$p < 0.01$, ***$p < 0.001$, ****$p < 0.0001$).

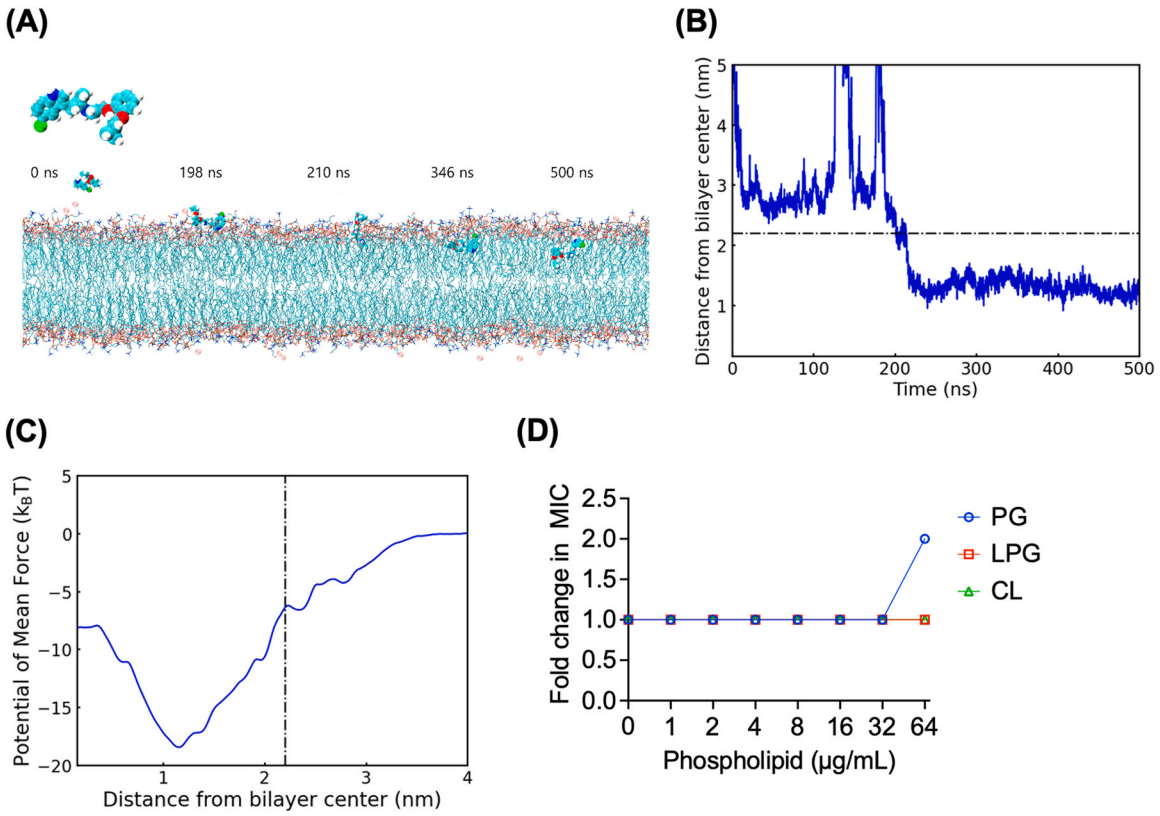


Fig. 3. All-atom molecular dynamics (MD) simulation and phospholipid binding assay reveal RS17053 interactions with phospholipid membranes. (A) Representative modeled arrangements of RS17053 interacting with a 7:3 DOPC/DOPG lipid bilayer, illustrating its progression from initial binding and penetration to final stabilization within the bilayer. RS17053 and sodium ions are depicted as large spheres; phospholipids are represented as chains. Atom colors are as follows: hydrogen (white), oxygen (red), nitrogen (blue), chlorine (green), carbon (cyan), phosphorus (orange), and sodium (pink). Water molecules are omitted for clarity. A zoomed-in view highlights the RS17053 structure within the bilayer. (B) Time evolution of the center-of-mass (COM) distance between RS17053 and the lipid bilayer during the MD simulation. (C) Free energy profile of RS17053 traversing the lipid bilayer, plotted against the bilayer COM distance. In panels (B) and (C), the dot-dashed black lines indicate the membrane interface. (D) Effect of phospholipids on RS17053 activity. MIC changes of RS17053 were evaluated in the presence of phosphatidylglycerol (PG), lysyl-phosphatidylglycerol (LPG), or cardiolipin (CL) using checkerboard microdilution assays. Phospholipid concentrations ranged from 0 to 64 μg/mL. Ciprofloxacin served as the negative control. The experiment was performed in triplicate, with all replicates showing consistent MIC changes.

cyclopropylmethoxyphenyl moiety interacts with lipid tails, facilitating deeper insertion into the bilayer (Fig. 3A, Video S1). Over time, these hydrophobic interactions overcome the initial electrostatic forces, allowing RS17053 to penetrate beyond the polar head groups and into the lipid interior. The chlorine substituent enhances lipophilicity, further promoting stable integration within the hydrophobic core of the bilayer.

Supplementary material related to this article can be found online at doi:10.1016/j.biopha.2025.118763.

Time-evolution analysis of the position of RS17053 relative to the bilayer center revealed that RS17053 remains near the membrane surface for the first ~200 ns, undergoing transient interactions with lipid head groups (Fig. 3B). After this period, RS17053 fully inserts into the bilayer and stabilizes within the hydrophobic region (Fig. 3B), indicating successful membrane penetration. The potential of mean force profile supports this finding, showing a favorable energy minimum at ~1 nm from the bilayer center, suggesting that RS17053 preferentially localizes within the membrane (Fig. 3C). The energy barrier for membrane exit further indicates that, once embedded, RS17053 remains stably associated with the lipid environment.

To experimentally validate the interaction between RS17053 and bacterial phospholipids, we assessed its binding affinity to key phospholipid components of the *S. aureus* membrane, including PG, lysyl-phosphatidylglycerol (LPG), and cardiolipin (CL). The MIC of RS17053 remained unchanged in the presence of LPG or CL (up to 64 μg/mL) (Fig. 3D). However, in the presence of 64 μg/mL PG, the MIC significantly increased (Fig. 3D), indicating a strong interaction between RS17053 and PG. This finding is consistent with the MD simulation results, which showed preferential binding to negatively charged DOPG. Together, these computational and experimental results demonstrate that RS17053 integrates into bacterial membranes by interacting with phospholipids, disrupting lipid organization, and potentially compromising membrane stability, which may contribute to its antimicrobial activity.

3.5. *RS17053 eradicates MRSA persisters via membrane disruption*

Considering that certain membrane-disrupting agents can effectively kill bacterial persisters, we evaluated whether RS17053 exhibits similar activity against MRSA persisters. Stationary-phase and arsenate-induced persisters of *S. aureus* MW2 were generated using established methods [4,17,28]. Their nonreplicating state and antibiotic tolerance were confirmed by the absence of viability reduction following a 4-h treatment with 100 × MIC vancomycin, gentamicin, or ciprofloxacin (Fig. 4A, B).

RS17053 showed potent, dose-dependent activity against diverse MRSA persisters. Although the FDA-approved membrane-targeting antibiotic daptomycin at 64 μg/mL reduced stationary-phase MRSA persisters by approximately 1 log, RS17053 resulted in a 3-log reduction at 32 μg/mL and completely eradicated the persisters at a density of 2×10^8 CFU/mL at 64 μg/mL within 4 h (Fig. 4A). This compound also eliminated arsenate-induced MRSA persisters at 32 μg/mL within 3 h

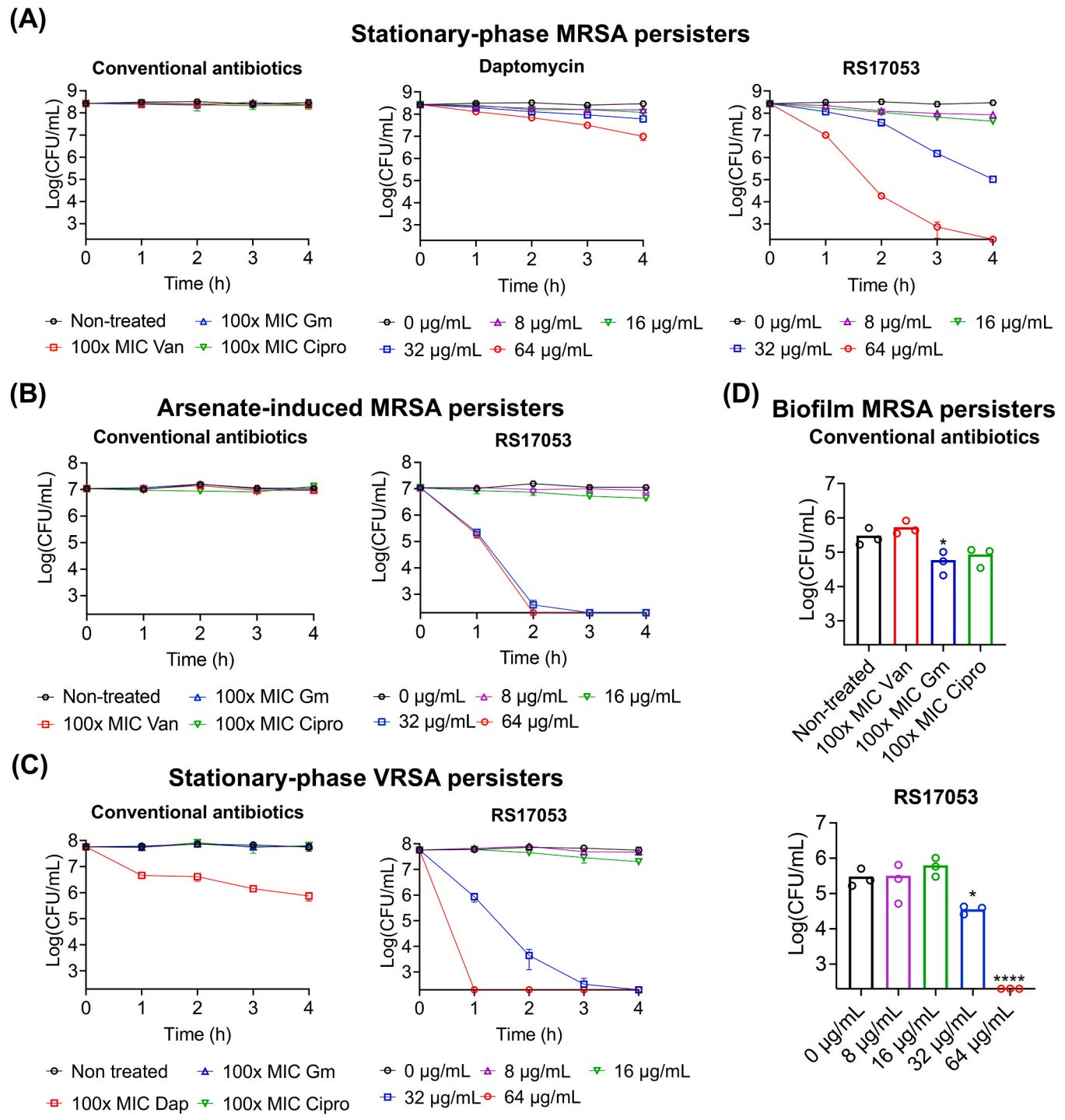


Fig. 4. RS17053 eradicates MRSA persister cells. Viability of (A) stationary-phase persisters and (B) arsenate-induced persisters from the MRSA strain MW2, and (C) stationary-phase persisters from the VRSA strain VRS1 following 4-h treatment with vancomycin (Van), gentamicin (Gm), ciprofloxacin (Cipro), daptomycin (Dap), or RS17053 at the indicated concentrations. Data points on the x-axis fall below the detection limit (2×10^2 CFU/mL). Error bars represent mean ± SD (n = 3). (D) Viability of MRSA MW2 biofilm persister cells after 24-h treatment with 100 × MIC of vancomycin (Van), gentamicin (Gm), ciprofloxacin (Cipro), or varying concentrations of RS17053. Data points on the x-axis are below the detection threshold (2×10^2 CFU/mL). Individual data points represent a biologically independent sample, with error bars indicating mean ± SD (n = 3). Statistical significance was determined using one-way ANOVA followed by Tukey's post-hoc test (*$p < 0.05$, **** $p < 0.0001$).

(Fig. 4B). Similarly, although daptomycin achieved only a 1.5-log reduction in VRSA persisters, RS17053 completely eradicated them at 32 μg/mL within 4 h (Fig. 4C). Furthermore, RS17053 eliminated MRSA persisters embedded in mature biofilms at 64 μg/mL (Fig. 4D).

To investigate the mechanism underlying its persister-killing activity, we examined the effects of RS17053 on membrane integrity. Daptomycin, which exhibited limited killing potency, did not induce SYTOX Green uptake or cause leakage of intracellular ATP and proteins, suggesting it does not permeabilize persister membranes (Fig. 5A). In contrast, RS17053 triggered rapid SYTOX Green uptake and induced ATP leakage in a dose-dependent manner at concentrations of 16 μg/mL or higher (Fig. 5B). In addition, intracellular protein leakage was

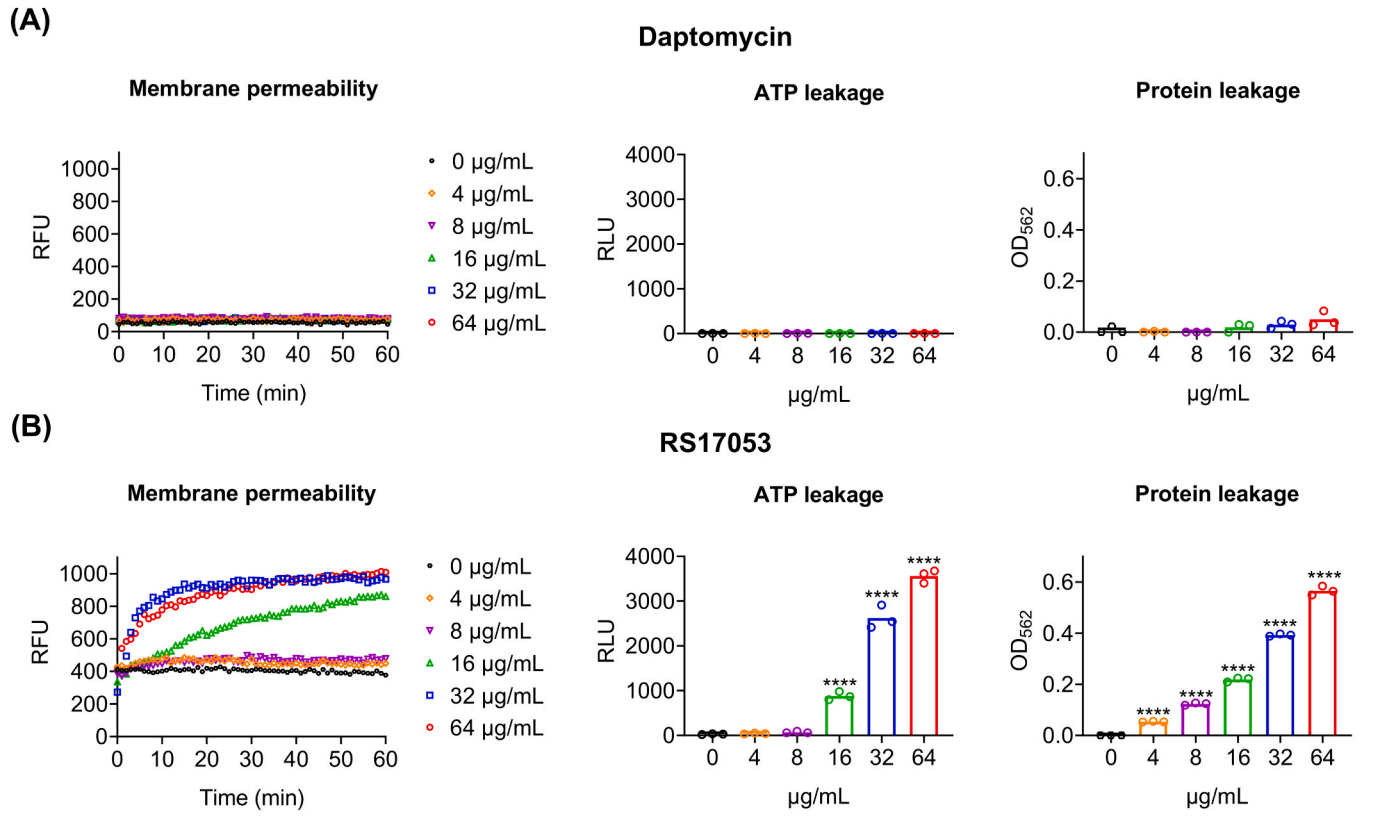


Fig. 5. RS17053 disrupts MRSA persister membranes. MRSA MW2 persister cells were treated with the indicated concentrations of (A) daptomycin and (B) RS17053. Membrane permeability was assessed by measuring SYTOX Green uptake over 60 min; data represent the mean of three independent experiments. ATP and protein leakage were quantified 1 h post-treatment using ATP luminescence and micro-BCA protein assays, respectively. Individual data points represent biologically independent samples, with error bars indicating mean ± SD (n = 3). Statistical significance was determined using one-way ANOVA followed by Tukey's post-hoc test (****$p < 0.0001$).

observed at concentrations as low as 4 μg/mL (Fig. 5B). These findings indicate that RS17053 kills MRSA and VRSA persisters by disrupting membrane integrity, leading to the loss of cellular contents and collapse of metabolic homeostasis.

3.6. *RS17053 selectively targets bacterial over mammalian membranes*

We investigated whether RS17053 selectively disrupts bacterial membranes while sparing mammalian cells. Hemolytic activity assays revealed no detectable hemolysis of human RBCs at concentrations up to 64 μg/mL. Moreover, only approximately 4.5 % hemolysis was observed at 128 μg/mL (Fig. 6A). To further assess mammalian cell membrane integrity, we measured ATP leakage from A549 human lung epithelial cells and AML12 mouse hepatocytes. The cationic surfactant benzyldimethylhexadecylammonium chloride (16-BAC) caused substantial ATP leakage at 64 μg/mL, whereas RS17053 induced no detectable leakage in A549 cells and only minor leakage in AML12 cells at concentrations of 16 μg/mL or higher, markedly less than that caused by 16-BAC (Fig. 6B).

Next, we examined the interaction of RS17053 with major lipid components of mammalian membranes, phosphatidylcholine (PC) and cholesterol (Chol) [29]. As shown in Fig. 6C, the MIC of RS17053 against *S. aureus* MW2 remained unchanged in the presence of either PC or Col up to 64 μg/mL, in contrast to its increased MIC in the presence of the bacterial membrane lipid PG (Fig. 3D). These results indicate that RS17053 selectively interacts with the anionic phospholipid PG, which is abundant in bacterial membranes but absent in mammalian membranes. Together, these findings support that RS17053 exerts its membrane activity through preferential binding to bacterial, rather than mammalian, membrane components.

In vivo toxicity was assessed using *Caenorhabditis elegans*, a well-established model organism for chemical toxicity evaluation [30]. RS17053 caused no detectable reduction in worm survival at concentrations up to 16 μg/mL. A modest but significant decrease was observed at 32 μg/mL, with a further reduction at 64 μg/mL compared with the 0.1 % DMSO control (Fig. 6D). Notably, more than 50 % of the worms survived even at the highest concentration tested, indicating a median lethal concentration (LC_{50}) exceeding 64 μg/mL (Fig. 6C). Considering both the MIC and the concentration that fully protect MRSA-infected worms are 8 μg/mL (Fig. 1C), RS17053 exhibits a selectivity index of at least eightfold, which is within the range reported for other early-stage membrane-active leads [31–33]. Taken together, these results indicate that RS17053 selectively targets bacterial membranes and is generally well tolerated at or near its antimicrobial MIC, with measurable toxicity only at higher concentrations.

3.7. *RS17053 enhances aminoglycoside uptake in MRSA persister cells*

Because RS17053 increases membrane permeability in MRSA persisters, we tested whether it promotes aminoglycoside uptake. Measuring intracellular GTTR accumulation revealed a dose-dependent increase in red fluorescence in RS17053-treated persisters (Fig. 7A), consistent with enhanced uptake.

Aminoglycoside tolerance in MRSA persisters is largely owing to diminished PMF, which is necessary for drug uptake. Given that RS17053 promotes aminoglycoside entry, we hypothesized that it would potentiate aminoglycoside-mediated killing. Indeed, while 8 μg/mL RS17053 or 10 μg/mL gentamicin alone failed to kill MRSA persisters, their combination resulted in a 5-log reduction in persister viability within 4 h. Similarly, although 5 μg/mL tobramycin alone had no effect on persister viability, when combined with 8 μg/mL RS17053, it also

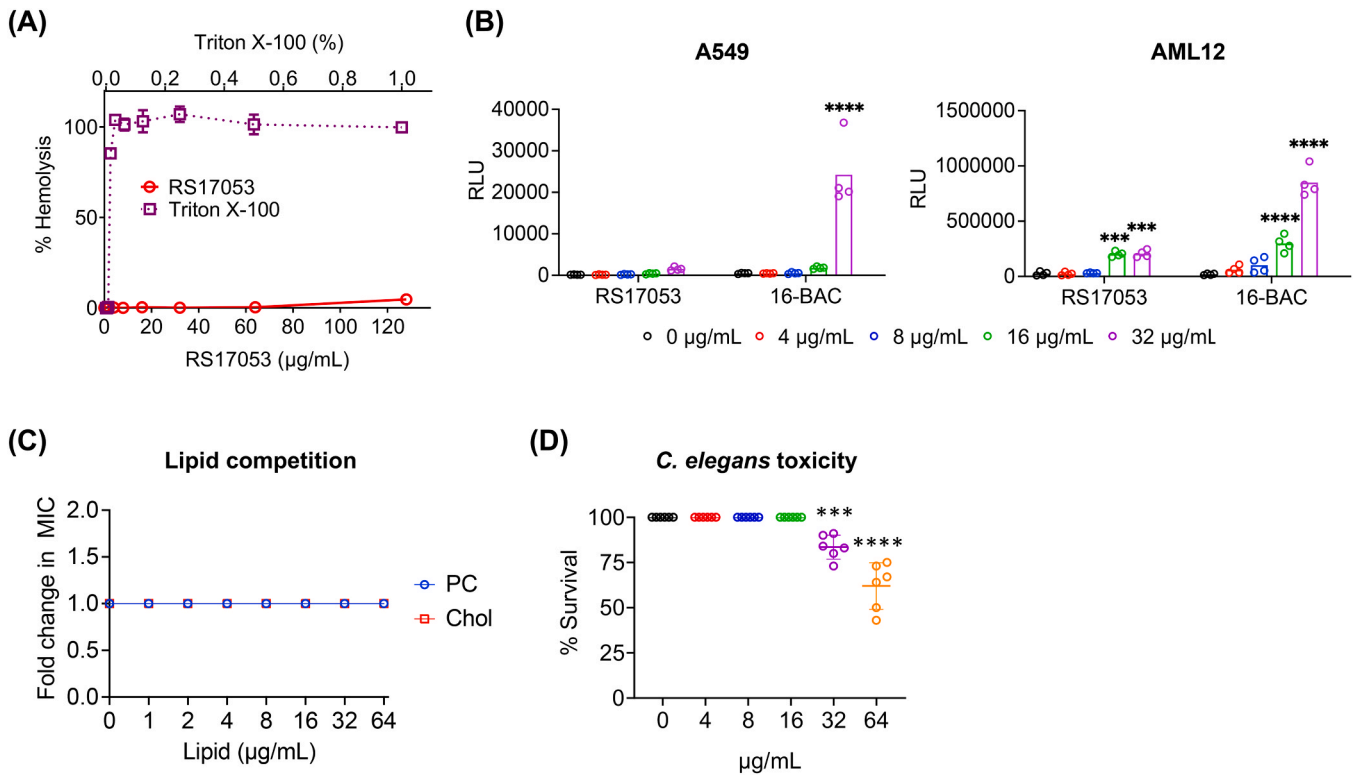


Fig. 6. RS17053 exhibits selectivity for bacterial over mammalian membranes. (A) Hemolytic activity of RS17053 was evaluated by incubating 2 % human red blood cells with increasing concentrations of RS17053 or 1 % Triton X-100 as a positive control for 1 h at 37°C. Complete hemolysis induced by 1 % Triton X-100 served as the reference. Data represent the mean of three independent experiments, with error bars indicating mean ± SD (n = 3). (B) Membrane disruption in A549 human lung epithelial cells and AML12 mouse hepatocytes was assessed by measuring intracellular ATP leakage following RS17053 treatment using an ATP luminescence assay. The cationic surfactant benzyldimethylhexadecylammonium (16-BAC) served as a positive control. Error bars represent mean ± SD (n = 4). Statistical significance was determined using two-way ANOVA followed by Tukey's post-hoc test. (C) Effect of membrane lipids on RS17053 activity. The MIC of RS17053 was determined in the presence of phosphatidylcholine (PC) or cholesterol (Chol) using checkerboard microdilution assays. Lipid concentrations ranged from 0 to 64 μg/mL. Experiments were performed in triplicate, with all replicates showing consistent MIC results. (D) *In vivo* toxicity of RS17053 was examined using *Caenorhabditis elegans* lethality as an endpoint over a 5-day period, with 0.1 % DMSO as a vehicle control. Error bars represent mean ± SD (n = 6). Statistical significance was determined using one-way ANOVA followed by Tukey's post-hoc test. For Panels (B) and (C), ***$P < 0.001$, ****$P < 0.0001$.

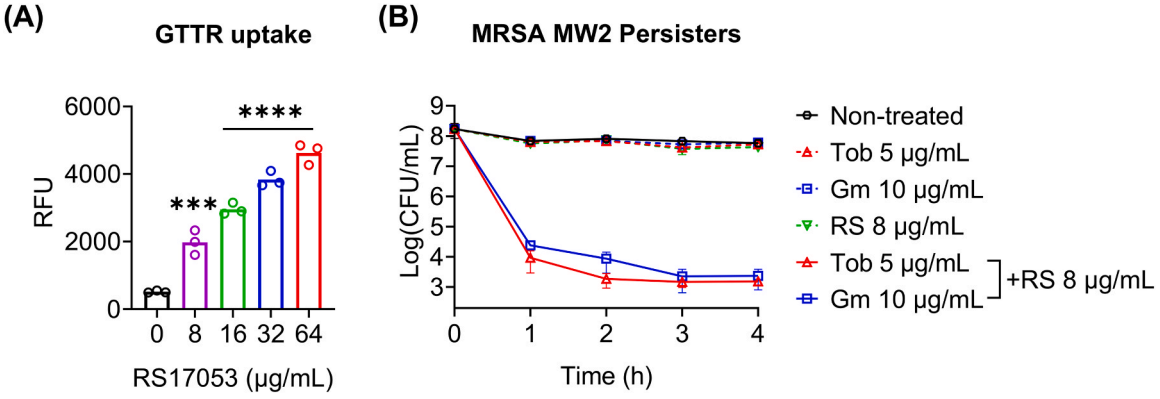


Fig. 7. RS17053 exhibits synergistic bactericidal activity with aminoglycosides against MRSA persisters. (A) Uptake of Texas Red–gentamicin conjugate (GTTR) by stationary-phase MRSA MW2 persisters was measured 1 h after treatment with the indicated concentrations of RS17053. Data represent biologically independent samples, with error bars indicating mean ± SD (n = 3). Statistical significance was determined using one-way ANOVA followed by Tukey's post-hoc test (***p < 0.001, ****p < 0.0001). (B) Viability of MRSA persisters following 4-h treatment with RS17053 either alone or in combination with gentamicin (Gm) or tobramycin (Tob) at the indicated concentrations. Viability was determined by quantifying colony-forming units (CFUs) through serial dilution and plating on CaMH agar plates. Data points represent biologically independent samples, with error bars indicating mean ± SD (n = 3).

induced a 5-log reduction in persister viability within 4 h. In time-kill kinetic assays, synergy is defined as a ≥ 2-log reduction in CFU/mL when a combination treatment is compared with the most active single agent [18]. By this criterion, RS17053 acts as a synergistic adjuvant with aminoglycosides, restoring bactericidal activity against MRSA persisters.

4. Discussion

Eradication of persister cells is essential for resolving chronic MRSA

infections, yet most existing antibiotics fail because they primarily target biosynthetic pathways that are largely inactive in dormant cells. RS17053 addresses this therapeutic gap by directly compromising membrane integrity—a growth-independent vulnerability—thereby eliminating both replicating and dormant MRSA. Importantly, its low propensity for resistance development, selective activity toward bacterial membranes, and ability to synergize with aminoglycosides highlight its potential as an antimicrobial lead.

Our computational and biochemical analyses suggest that RS17053's membrane-targeting activity arises from the combined action of electrostatic and hydrophobic forces. The indole NH group likely initiates electrostatic binding to anionic phospholipids such as PG, while the cyclopropylmethoxyphenyl moiety and chlorine substituent drive hydrophobic insertion into the bilayer. This mechanistic framework offers a clear rationale for medicinal chemistry optimization. For example, introducing cationic groups onto the indole scaffold could enhance electrostatic anchoring to bacterial membranes while reducing nonspecific interactions with the predominantly zwitterionic membranes of mammalian cells [34–36]. Alternatively, fine-tuning hydrophobicity—via halogen substitution or expansion of the cyclopropylmethoxyphenyl moiety—may strengthen bilayer insertion and improve potency [33,37,38]. Such strategies have proven effective in optimizing other membrane-active agents, including synthetic retinoids and nTZDpa derivatives [17,33], and could likewise enhance the safety and efficacy of RS17053.

An interesting observation is the significant synergy between RS17053 and aminoglycosides against persisters, but not against actively growing MRSA. This difference likely reflects fundamental distinctions in aminoglycoside uptake. In growing cells, uptake is driven efficiently by PMF, so additional membrane permeabilization confers little benefit. In contrast, persisters have a diminished PMF, which limits aminoglycoside entry. By permeabilizing the membrane, RS17053 nullifies this barrier, facilitating rapid aminoglycoside uptake and restoring bactericidal activity. This finding highlights the need to evaluate antibiotic combinations in both replicating and dormant bacterial populations, as standard MIC-based synergy assays may underestimate clinically relevant interactions in persistent infections.

Clinically, aminoglycosides remain valuable for treating biofilm-associated MRSA infections, but effective dosing often requires high, prolonged exposure due to poor biofilm penetration and antibiotic tolerance. Such regimens increase the risk of nephrotoxicity and accelerate resistance development [39–43]. The ability of RS17053 to restore aminoglycoside activity against persisters suggests a potential role as an adjuvant, enabling lower aminoglycoside doses while maintaining therapeutic efficacy. Because RS17053 and aminoglycosides act on distinct targets—membrane disruption and ribosomal inhibition—their combination may also reduce selective pressure on any single pathway, potentially limiting resistance emergence. This dose-sparing and resistance-mitigating effect could improve the safety of aminoglycoside therapy while broadening RS17053's own therapeutic window for treating persistent MRSA infections.

While RS17053 demonstrates potent activity against MRSA persisters and uniquely enhances aminoglycoside uptake, further studies are required to address its limitations and better define its potential as an antimicrobial lead. Key priorities include structure–activity relationship (SAR) optimization to improve antimicrobial potency and bacterial selectivity, reduce cytotoxicity, and eliminate its inherent α1A-adrenoceptor antagonistic activity. These efforts should be followed by pharmacokinetic and safety evaluations in mammalian models, with particular emphasis on biofilm-associated and chronic infection settings where persister populations predominate. Addressing these aspects will be essential to delineate the therapeutic window of RS17053 and inform its future development.

5. Conclusion

We identify RS17053, a repurposed α1A-adrenoceptor antagonist, as a membrane-disrupting agent that eradicates MRSA persisters, enhances aminoglycoside uptake, and confers *in vivo* protection. Its selective action on bacterial membranes, low propensity for resistance development, and synergy with aminoglycosides position RS17053 as a compelling lead compound for antimicrobial strategies targeting persistent MRSA infections.

Author Contributions

W.K. conceived, designed, and coordinated the overall study. S.B., N. L., J.K., J.K., and W.K. performed the experiments and analyses. G.Z. and H.G. designed, performed, and analyzed the MD simulations. J.K., W.S., H.G., and W.K. contributed reagents, materials, and analysis tools. H.G. and W.K. acquired funding. S.B., G.Z., H.G., and W.K. wrote the manuscript. W.K. supervised the project. All authors read and approved the final version of the manuscript.

CRediT authorship contribution statement

Huajian Gao: Writing – review & editing, Writing – original draft, Validation, Resources, Methodology, Formal analysis, Data curation. **Wonhyo Seo:** Writing – review & editing, Resources, Methodology, Formal analysis. **Jae-Seok Kim:** Writing – review & editing, Validation, Resources, Methodology. **Jisoo Kang:** Writing – review & editing, Validation, Methodology, Investigation, Data curation. **Nakyung Lee:** Writing – review & editing, Validation, Methodology, Investigation, Formal analysis, Data curation. **Guijin Zou:** Writing – review & editing, Writing – original draft, Visualization, Validation, Methodology, Investigation, Formal analysis, Data curation. **Seongeun Baek:** Writing – review & editing, Writing – original draft, Validation, Methodology, Investigation, Formal analysis, Data curation. **Wooseong Kim:** Writing – review & editing, Writing – original draft, Validation, Supervision, Resources, Methodology, Investigation, Funding acquisition, Formal analysis, Data curation, Conceptualization.

Declaration of Competing Interest

The authors of this manuscript declare no conflicts of interest.

Acknowledgments

This work was supported by a grant from the National Research Foundation of Korea (NRF), funded by the Korean government (MSIT) (NRF-RS-2023–00228746). The experimental equipment was supported by a Korea Basic Science Institute (National research Facilities and Equipment Center) grant (2021R1A6C101A442).

Appendix A. Supporting information

Supplementary data associated with this article can be found in the online version at doi:10.1016/j.biopha.2025.118763.

Data availability

Data will be made available on request.

References

[1] A.S. Lee, H. de Lencastre, J. Garau, J. Kluytmans, S. Malhotra-Kumar, A. Peschel, S. Harbarth, Methicillin-resistant Staphylococcus aureus, Nat. Rev. Dis. Prim. 4 (2018) 18033, https://doi.org/10.1038/nrdp.2018.33.

[2] G.B.D. 2021 Antimicrobial Resistance Collaborators, Global burden of bacterial antimicrobial resistance 1990–2021: a systematic analysis with forecasts to 2050, Lancet 404 (2024) 1199–1226, https://doi.org/10.1016/s0140-6736(24)01867-1.

[3] C.-J. Chen, Y.-C. Huang, S.-S. Shie, Evolution of multi-resistance to vancomycin, daptomycin, and linezolid in methicillin-resistant staphylococcus aureus causing persistent bacteremia, Front. Microbiol 11 (2020) 1414, https://doi.org/10.3389/fmicb.2020.01414.
[4] B.P. Conlon, S.E. Rowe, A.B. Gandt, A.S. Nuxoll, N.P. Donegan, E.A. Zalis, G. Clair, J.N. Adkins, A.L. Cheung, K. Lewis, Persister formation in Staphylococcus aureus is associated with ATP depletion, Nat. Microbiol. 1 (2016) 16051, https://doi.org/10.1038/nmicrobiol.2016.51.
[5] F. Peyrusson, H. Varet, T.K. Nguyen, R. Legendre, O. Sismeiro, J.-Y. Coppée, C. Wolz, T. Tenson, F.V. Bambeke, Intracellular Staphylococcus aureus persisters upon antibiotic exposure, Nat. Commun. 11 (2020) 2200–2214, https://doi.org/10.1038/s41467-020-15966-7.
[6] H. Niu, J. Gu, Y. Zhang, Bacterial persisters: molecular mechanisms and therapeutic development, Signal Transduct. Target. Ther. 9 (2024) 174, https://doi.org/10.1038/s41392-024-01866-5.
[7] K.R. Allison, M.P. Brynildsen, J.J. Collins, Metabolite-enabled eradication of bacterial persisters by aminoglycosides, Nature 473 (2011) 216–220, https://doi.org/10.1038/nature10069.
[8] W. Kim, G. Zou, T.P.A. Hari, I.K. Wilt, W. Zhu, N. Galle, H.A. Faizi, G.L. Hendricks, K. Tori, W. Pan, X. Huang, A.D. Steele, E.E. Csatary, M.M. Dekarske, J.L. Rosen, N. de, Q. Ribeiro, K. Lee, J. Port, B.B. Fuchs, P.M. Vlahovska, W.M. Wuest, H. Gao, F.M. Ausubel, E. Mylonakis, A selective membrane-targeting repurposed antibiotic with activity against persistent methicillin-resistant Staphylococcus aureus, Proc. Natl. Acad. Sci. USA 116 (2019) 16529–16534, https://doi.org/10.1073/pnas.1904700116.
[9] J.G. Hurdle, A.J. O'Neill, I. Chopra, R.E. Lee, Targeting bacterial membrane function: an underexploited mechanism for treating persistent infections, Nat. Rev. Microbiol. 9 (2011) 62–75, https://doi.org/10.1038/nrmicro2474.
[10] R.M. Epand, C. Walker, R.F. Epand, N.A. Magarvey, Molecular mechanisms of membrane targeting antibiotics, Biochim. Biophys. Acta 1858 (2016) 980–987, https://doi.org/10.1016/j.bbamem.2015.10.018.
[11] S.A. Alghareeb, J. Alsughayyir, M.A. Alfhili, Stimulation of hemolysis and eryptosis by α-mangostin through Rac1 GTPase and oxidative injury in human red blood cells, Molecules 28 (2023) 6495, https://doi.org/10.3390/molecules28186495.
[12] W. Kim, N. Fricke, A.L. Conery, B.B. Fuchs, R. Rajamuthiah, E. Jayamani, P. M. Vlahovska, F.M. Ausubel, E. Mylonakis, NH125 kills methicillin-resistant Staphylococcus aureus persisters by lipid bilayer disruption, Future Med. Chem. 8 (2016) 257–269, https://doi.org/10.4155/fmc.15.189.
[13] S. Lechner, K. Lewis, R. Bertram, Staphylococcus aureus persisters tolerant to bactericidal antibiotics, J. Mol. Microbiol. Biotechnol. 22 (2012) 235–244, https://doi.org/10.1159/000342449.
[14] H.Y. Heo, G. Zou, S. Baek, J. Kim, E. Mylonakis, F.M. Ausubel, H. Gao, W. Kim, A Methylazanediyl bisacetamide derivative sensitizes staphylococcus aureus persisters to a combination of gentamicin and daptomycin, Adv. Sci. 11 (2024) 2306112, https://doi.org/10.1002/advs.202306112.
[15] W. Kim, G. Zou, W. Pan, N. Fricke, H.A. Faizi, S.M. Kim, R. Khader, S. Li, K. Lee, I. Escorba, P.M. Vlahovska, H. Gao, F.M. Ausubel, E. Mylonakis, M.J. Blaser, The neutrally charged diarylurea compound PQ401 kills antibiotic-resistant and antibiotic-tolerant staphylococcus aureus, mBio 11 (2020) 603, https://doi.org/10.1128/mbio.01140-20.
[16] C. and L.S.. Institute, Methods for dilution antimicrobial susceptibility tests for bacteria that grow aerobically; approved standard-ninth edition. CLSI document M07-A9., 2012.
[17] W. Kim, W. Zhu, G.L. Hendricks, D.V. Tyne, A.D. Steele, C.E. Keohane, N. Fricke, A. L. Conery, S. Shen, W. Pan, K. Lee, R. Rajamuthiah, B.B. Fuchs, P.M. Vlahovska, W. M. Wuest, M.S. Gilmore, H. Gao, F.M. Ausubel, E. Mylonakis, A new class of synthetic retinoid antibiotics effective against bacterial persisters, Nature 556 (2018) 103–107, https://doi.org/10.1038/nature26157.
[18] C.D. Doern, When does 2 plus 2 equal 5? A review of antimicrobial synergy testing, J. Clin. Microbiol. 52 (2014) 4124–4128, https://doi.org/10.1128/jcm.01121-14.
[19] S.M. Kim, G. Zou, H. Kim, M. Kang, S. Ahn, H.Y. Heo, J.-S. Kim, K.-M. Lim, F. M. Ausubel, E. Mylonakis, H. Gao, W. Kim, Antimicrobial activity of the membrane-active compound nTZDpa is enhanced at low pH, Biomed. Pharmacother. 150 (2022) 112977, https://doi.org/10.1016/j.biopha.2022.112977.
[20] N. Chandal, R. Kalia, A. Dey, R. Tambat, N. Mahey, S. Jachak, H. Nandanwar, Synthetic indole derivatives as an antibacterial agent inhibiting respiratory metabolism of multidrug-resistant gram-positive bacteria, Commun. Biol. 7 (2024) 1489, https://doi.org/10.1038/s42003-024-06996-8.
[21] A.P. Ford, N.F. Arredondo, J.D.R. Blue, D.W. Bonhaus, J. Jasper, M.S. Kava, J. Lesnick, J.R. Pfister, I.A. Shieh, R.L. Vimont, T.J. Williams, J.E. McNeal, T. A. Stamey, D.E. Clarke, RS-17053 (N-[2-(2-cyclopropylmethoxyphenoxy)ethyl]-5-chloro-alpha, alpha-dimethyl-1H-indole-3-ethanamine hydrochloride), a selective alpha 1A-adrenoceptor antagonist, displays low affinity for functional alpha 1-adrenoceptors in human prostate: implications for adrenoceptor classification, Mol. Pharmacol. 49 (1996) 209–215.
[22] P.J. Wellman, L.R. McMAHON, T. Green, A. Tole, Effects of the α1a-adrenoceptor antagonist RS-17053 on phenylpropanolamine-induced anorexia in rats, Pharmacol. Biochem. Behav. 57 (1997) 281–284, https://doi.org/10.1016/s0091-3057(96)00351-6.
[23] H.A. Alsufyani, J.R. Docherty, Effects of RS17053 on α1-adrenoceptors in rat vas deferens and aorta, Fundam. Clin. Pharmacol. 37 (2023) 1170–1178, https://doi.org/10.1111/fcp.12930.
[24] C.D. Sifri, J. Begun, F.M. Ausubel, S.B. Calderwood, Caenorhabditis elegans as a model host for Staphylococcus aureus pathogenesis, Infect. Immun. 71 (2003) 2208–2217, https://doi.org/10.1128/iai.71.4.2208-2217.2003.
[25] C.L. Friedrich, D. Moyles, T.J. Beveridge, R.E. Hancock, Antibacterial action of structurally diverse cationic peptides on Gram-positive bacteria, Antimicrob. Agents Chemother. 44 (2000) 2086–2092, https://doi.org/10.1128/aac.44.8.2086-2092.2000.
[26] P.-L. Lam, R.S.-M. Wong, K.-H. Lam, L.-K. Hung, M.-M. Wong, L.-H. Yung, Y.-W. Ho, W.-Y. Wong, D.K.-P. Hau, R. Gambari, C.-H. Chui, The role of reactive oxygen species in the biological activity of antimicrobial agents: an updated mini review, Chem. Biol. Interact. 320 (2020) 109023, https://doi.org/10.1016/j.cbi.2020.109023.
[27] Y.-F. Chen, T.-L. Sun, Y. Sun, H.W. Huang, Interaction of daptomycin with lipid bilayers: a lipid extracting effect, Biochemistry 53 (2014) 5384–5392, https://doi.org/10.1021/bi500779g.
[28] S. Baek, J. Seo, T. Yun, J. Kim, Y. Shin, J. Choi, J. Chang, I. Kim, Y.-H. Yang, W. Kim, W. Lee, Heavy metals promote the formation of multidrug-tolerant Staphylococcus aureus and Escherichia coli persisters, Ecotoxicol. Environ. Saf. 293 (2025) 118014, https://doi.org/10.1016/j.ecoenv.2025.118014.
[29] G. van Meer, D.R. Voelker, G.W. Feigenson, Membrane lipids: where they are and how they behave, Nat. Rev. Mol. Cell Biol. 9 (2008) 112–124, https://doi.org/10.1038/nrm2330.
[30] P.R. Hunt, The C. elegansmodel in toxicity testing, J. Appl. Toxicol. 37 (2016) 50–59, https://doi.org/10.1002/jat.3357.
[31] I. Orme, T.D.S. program, search for new drugs for treatment of tuberculosis, Antimicrob. Agents Chemother. 45 (2001) 1943–1946, https://doi.org/10.1128/aac.45.7.1943-1946.2001.
[32] B. Wang, B. Pachaiyappan, J.D. Gruber, M.G. Schmidt, Y.-M. Zhang, P.M. Woster, Antibacterial diamines targeting bacterial membranes, J. Med. Chem. 59 (2016) 3140–3151, https://doi.org/10.1021/acs.jmedchem.5b01912.
[33] W. Kim, A.D. Steele, W. Zhu, E.E. Csatary, N. Fricke, M.M. Dekarske, E. Jayamani, W. Pan, B. Kwon, I.F. Sinitsa, J.L. Rosen, A.L. Conery, B.B. Fuchs, P.M. Vlahovska, F.M. Ausubel, H. Gao, W.M. Wuest, E. Mylonakis, Discovery and optimization of nTZDpa as an antibiotic effective against bacterial persisters, ACS Infect. Dis. 4 (2018) 1540–1545, https://doi.org/10.1021/acsinfecdis.8b00161.
[34] C. Ghosh, J. Haldar, Membrane-active small molecules: designs inspired by antimicrobial peptides, ChemMedChem 10 (2015) 1606–1624, https://doi.org/10.1002/cmdc.201500299.
[35] R. Yang, W. Cheng, M. Huang, T. Xu, M. Zhang, J. Liu, S. Qin, Y. Guo, Novel membrane-targeting isoxanthohumol-amine conjugates for combating methicillin-resistant Staphylococcus aureus (MRSA) infections, Eur. J. Med. Chem. 268 (2024) 116274, https://doi.org/10.1016/j.ejmech.2024.116274.
[36] J. Oh, S.-M. Choi, Y. Yun, J. Choi, A.E. Barron, K.-H. Park, J. Seo, Local enhancement of cationic charge density via polyamine side chain incorporation improves the selectivity of antimicrobial peptoids, Eur. J. Med. Chem. 297 (2025) 117920, https://doi.org/10.1016/j.ejmech.2025.117920.
[37] A. Sharma, S.J. Jain, P.N. Jha, S. Rudrawar, S.B. Bharate, H.R. Jadhav, Unfolding the potential of pyrrole- and indole-based allylidene hydrazine carboximidamides as antimicrobial agents, ACS Infect. Dis. 11 (2025) 493–505, https://doi.org/10.1021/acsinfecdis.4c00849.
[38] H. Huo, W. Dan, M. Li, Y. Chen, C. Yang, L. Wu, B. Shi, J. Li, Design, synthesis, and biological evaluation of steroidal indole derivatives as membrane-targeting antibacterial candidates, Eur. J. Med. Chem. 283 (2025) 117156, https://doi.org/10.1016/j.ejmech.2024.117156.
[39] D. Lebeaux, J.-M. Ghigo, C. Beloin, Biofilm-related infections: bridging the gap between clinical management and fundamental aspects of recalcitrance toward antibiotics, Microbiol. Mol. Biol. Rev. 78 (2014) 510–543, https://doi.org/10.1128/mmbr.00013-14.
[40] M.-P. Mingeot-Leclercq, P.M. Tulkens, Aminoglycosides: nephrotoxicity, Antimicrob. Agents Chemother. 43 (1999) 1003–1012, https://doi.org/10.1128/aac.43.5.1003.
[41] M. Al-Aloul, H. Miller, S. Alapati, P.A. Stockton, M.J. Ledson, M.J. Walshaw, Renal impairment in cystic fibrosis patients due to repeated intravenous aminoglycoside use, Pediatr. Pulmonol. 39 (2005) 15–20, https://doi.org/10.1002/ppul.20138.
[42] M.M. Moody, C.A. de Jongh, S.C. Schimpff, G.L. Tillman, Long-term amikacin use: effects on aminoglycoside susceptibility patterns of gram-negative bacilli, JAMA 248 (1982) 1199–1202, https://doi.org/10.1001/jama.1982.03330100037027.
[43] G. Millette, D.L. Séguin, C. Isabelle, S. Chamberland, J.-F. Lucier, S. Rodrigue, A. M. Cantin, F. Malouin, Staphylococcus aureus small-colony variants from airways of adult cystic fibrosis patients as precursors of adaptive antibiotic-resistant mutations, Antibiotics 12 (2023) 1069, https://doi.org/10.3390/antibiotics12061069.